

Effective action for bubble nucleation rates

Ian G. Moss and Wade Naylor*

Department of Physics, University of Newcastle Upon Tyne, NE1 7RU U.K.

(June 2001)

Abstract

We develop a method to calculate the prefactor in the expression for the bubble nucleation rate. A fermion with Yukawa coupling is considered where a step potential can be used as a good approximation in the thin wall limit. Corrections due to thicker walls are investigated by perturbing about the thin wall case. We derive the thermal one loop effective action, calculating it numerically, and find that the prefactor in the nucleation rate can both suppress and enhance, for a given temperature, when the usual renormalisation conditions are applied to the effective potential.

Pacs numbers: 03.70.+k, 98.80.Cq

Typeset using REVTeX

*Current address: Department of Earth & Space Science, Osaka University, OSAKA 560-0043, Japan

I. INTRODUCTION

Bubble nucleation can occur in a first order phase transition from the false to the true vacuum. The bubble nucleation rate per unit volume per unit time, written in the language of Coleman [1], is $\Gamma/V = A e^{-B}$, where B is the classical Euclidean action of the bubble and A is the one loop contribution including zero and negative modes.

The purpose of this paper is to present a method that enables one to calculate the nucleation rate in the thin wall limit. Techniques such as the derivative expansion break down for this type of background [7]. The thin wall limit is a possible scenario in electroweak theory with multiple Higgs fields [2]. It is also useful as a possible explanation for the generation of the baryon asymmetry we observe today [3]. In the interests of brevity we focus on just the fermion fields. However, the general discussion includes scalar and spinor fields for completeness. The calculation of other fields, using the method presented, is currently under way [4].

Previous work on nucleation rates includes an analysis of the prefactor for scalar fields coupled to fermions by Gleiser, Marques and Ramos [5], who computed the determinant using the derivative expansion. Issues regarding which loop corrections should be included in the bounce solution were investigated. Garriga [6] calculated the determinantal prefactor analytically, assuming the free energy can be approximated by that of a massless field living on the surface of a membrane. This was for a scalar field in the thin wall approximation (corrections due to thicker walls were also studied) at finite temperature, where enhancement of the nucleation rate was found. Kripfganz, Laser and Schmidt [7] computed the prefactor for the one loop Higgs fluctuations at the electroweak phase transition, using the derivative expansion as an approximation.

A particularly useful numerical method uses a theorem on functional determinants that can be found in Coleman's work [8]. Baacke and Kiselev [9] develop an 'exact' numerical scheme to work out the one loop corrections for a scalar field at finite temperature, using Coleman's theorem. Thick and thin walls were considered but an infinitely thin wall ($\alpha = 1$ in their notation) was not. Hence, there is no direct method of comparison with [6]. However, they also found an enhancement of the nucleation rate (depending on the choice of renormalisation scheme). Baacke [10] then studied vector bosons in the 't Hooft-Feynman gauge, generalising Coleman's theorem to the matrix case. The results were compared to those in [7], where there was good agreement for small (thick wall) bubbles and strong deviations between the results for large (thin wall) bubbles, as expected. The nucleation rate was suppressed for this case. Also, Baacke and Sürig [11] calculated the fermionic fluctuation determinant using Coleman's theorem and a gradient expansion for comparison. For an optimal choice of renormalisation, they found that the rate was enhanced at the electroweak temperature.

Brahm and Lee [12] used a different numerical procedure based on the phase shift method and similar to the one we shall employ (using some old results due to Schwinger [13]). They computed the prefactor for scalar fields at finite temperature for the thin wall limit, based on the assumption that the surface free energy is equal to that of a domain wall (thick walls were also considered). The WKB approximation was used for the high energy modes to improve convergence of the exact result. The results were compared with the effective potential and derivative expansion approximations (see references therein).

Further work has been done by Münster and Rotsch [14], who calculated the prefactor in the nucleation rate for a scalar field using a Pöschl-Teller potential and heat kernel coefficients to remove the ultraviolet divergences of the theory. Münster, Strumia and Tetradis [15] have compared this work to an entirely different method (not relying on saddle point evaluation) that uses coarse graining and renormalisation group techniques. They find good agreement between the two in the region of validity. Further work has been done using this coarse graining method and we refer the reader to [15] and the references therein.

In our method we shall use phase shifts and relate the prefactor to the heat kernel. The theory is regulated by subtracting off the relevant heat kernel coefficients. We consider fermions with a Yukawa coupling and a step function profile to begin with. Using the step function gives an exact analytic expression for the phase shift, making the calculation more manageable. For the fermion case, the thin wall limit introduces problems of its own because the derivative of the mass term leads to a delta function in the potential. As far as we are aware, this is the first time this specific case has been investigated, although the method used in [10] or [12] could be applied. Results are at finite temperature (not only in the high temperature limit) and the method can be extended to the zero temperature case. Also, the technique involves a simple regularisation step, unlike methods based on Coleman's theorem which require evaluating uniform asymptotic expansions of the relevant field equations.

The eigenvalues in the determinant are found using partial wave analysis and phase shifts, with the eigenmodes discretised by putting them in a sphere of large radius Ω that we let tend to infinity (not to be confused with the bubble wall radius at R). Thus, we must impose boundary conditions on the fields. In the case of fermions, the correct eigenvalue problem requires mixed boundary conditions (see appendix A).

The paper is organised as follows. In Sec. II A we relate the phase shift to the heat kernel and zeta function. In Sec. II B we calculate the thermal effective action leading to an expression for the prefactor in terms of the phase shift. In Sec. III we discuss how to consider corrections from thicker walls. In Sec. IV results are presented and in Sec. V we draw conclusions. In Sec. VI an appendix in three sections is given, with details on the calculation of the fermion phase shift, numerical zeta function regularisation and renormalisation respectively.

II. HEAT KERNELS AND PHASE SHIFTS

A. Nucleation & regularisation

We begin with the nucleation rates for the decay of a false vacuum at finite temperature due to an instanton ϕ_{bubble} . Any field that acquires a mass on the instanton background can contribute to the prefactor. In three dimensions [16] (see also comments in [5] & [12]),

$$A = T \left(\frac{B}{2\pi} \right)^{3/2} \prod_{fields} \left| \frac{det'[-\nabla^2 + m^2(\phi_{bubble})]}{det[-\nabla^2 + m^2(\phi_{sym})]} \right|^{-1/2}. \quad (1)$$

Three zero eigenvalues, arising from breaking the Poincare symmetry, each contribute $(B/2\pi)^{1/2}$ to the total and these are omitted from the scalar determinant, as indicated by the prime.

In the thin wall limit we assume that ϕ_{bubble} has a bubble wall at some radius R , such that ϕ takes the false vacuum value at radii $r > R$ and the true vacuum value at radii $r < R$, with a narrow transition region near $r = R$. For scalar bosons and fermions (and if calculated, the vector bosons), the relevant mass terms vanish in the false vacuum and are non-zero in the true vacuum, leading to a step function profile,

$$m(r) = \begin{cases} m & r < R \\ 0 & r > R \end{cases}. \quad (2)$$

In the same limit, the scalar Higgs field masses differ little for large and small radii. This suggests that the Higgs contribution to the prefactor is smaller than the fermion contribution (and also any other fields). We will consider the accuracy of the thin-wall approximation later.

The eigenvalues in the determinant can be found by using a partial wave analysis and phase shifts [17]. We first discretise the eigenmodes by putting them in a sphere of large radius Ω . After separating the eigenmodes into radial functions and spherical harmonics, the radial parts asymptotically approach trigonometric functions of $kr + \phi$, where ϕ is a constant phase depending on k and the angular momentum l . On the boundary,

$$k_n \Omega \approx n\pi - \phi. \quad (3)$$

In the false vacuum, the potential is zero and we label the free eigenvalues $k_n^{(0)}$

$$k_n^{(0)} \Omega \approx n\pi - \phi^{(0)}. \quad (4)$$

On letting $\Omega \rightarrow \infty$ (continuum limit), the above equations (3) and (4) imply a relationship between the phase shift $\delta_l(k) = \phi - \phi^{(0)}$, the density of states $g_l(k)$ and $g_l^{(0)}(k)$, [13],

$$g_l(k) = g_l^{(0)}(k) + \frac{1}{\pi} \frac{d\delta_l(k)}{dk}, \quad (5)$$

for the radial modes.

The difference between the heat kernels for the instanton and the true vacuum will be

$$\Delta K(t) = \sum_n \left(e^{-k_n^2 t} - e^{-k_n^{(0)2} t} \right) \quad (6)$$

Using the density of states factor $g_l(k)$ and the degeneracy factor χ_l ,

$$\Delta K(t) = \int_0^\infty dk e^{-k^2 t} \sum_l \chi_l (g_l(k) - g_l^{(0)}(k)). \quad (7)$$

Substituting (5) into the above equation and integrating by parts we obtain

$$\Delta K(t) = \frac{2}{\pi} \int_0^\infty dk e^{-k^2 t} kt \sum_l \chi_l \delta_l(k), \quad (8)$$

where the degeneracy factor $\chi_l = (2l + 1)$ in three dimensions.

The heat kernel can now be used to regularise the determinants appearing in the prefactor A in the nucleation rate. We define the generalised ζ function [18] by

$$\zeta(s) = \frac{1}{\Gamma(s)} \int_0^\infty t^{s-1} \text{tr} K(t) dt, \quad (9)$$

The analytic continuation of $\zeta(s)$ then gives

$$\log A = \sum_{\text{fields}} (\pm) \Delta W \quad (10)$$

where we take \pm for scalar and spinor fields respectively, and

$$\Delta W = \frac{1}{2} \zeta'(0) + \frac{1}{2} \zeta(0) \log \mu^2 \quad (11)$$

where μ is the renormalisation scale.

For numerical work, the analytic continuation can best be performed by subtracting terms from the heat kernel. As $t \rightarrow 0$, the heat kernel in $d+1$ dimensions has the asymptotic expansion [19]

$$K(t) \sim t^{-(d+1)/2} \sum_{n=0} B_n t^n. \quad (12)$$

The leading terms, which cause the poles in the ζ function, can be removed by replacing the sum over phase shifts in equation (8) by

$$\sum_l \chi_l \bar{\delta}_l = \sum_l \chi_l \delta_l - \frac{\pi B_1 k^{d-1}}{\Gamma(\frac{d+1}{2})} - \frac{\pi B_{3/2} k^{d-2}}{\Gamma(\frac{d}{2})} - \frac{\pi B_2 k^{d-3}}{\Gamma(\frac{d-1}{2})}, \quad (13)$$

where the B_0 coefficient cancels because it is equal to the free heat kernel $K^{(0)}$. An infrared cutoff M_{IR} must also be included, noting (see Appendix B) that the dependence on M_{IR} is illusory given that changing M_{IR} does not affect the value of ΔW . The $B_{3/2}$ coefficient only occurs for fermions because squaring the Dirac equation leads to a delta function in the potential (for a step profile). Heat kernel coefficients have been calculated for distributional backgrounds [20] and we only quote the result below.

For the step potential, standard expressions for the heat kernel coefficients give [19] (& [20]):

$$B_1 = -\frac{m^2 R^{d+1}}{2^d (d+1) \Gamma(\frac{d+1}{2})}, \quad (14)$$

$$B_{3/2} = \frac{m^2 R^d}{2^d \Gamma(\frac{d+1}{2})}, \quad (15)$$

$$B_2 = \frac{m^4 R^{d+1}}{2^{d+1} (d+1) \Gamma(\frac{d+1}{2})}. \quad (16)$$

For example, the phase shift [17] for a scalar boson field is

$$\tan \delta_l = \frac{k J_{l-1/2}(kR) J_{l+1/2}(k'R) - k' J_{l-1/2}(k'R) J_{l+1/2}(kR)}{k N_{l-1/2}(kR) J_{l+1/2}(k'R) - k' J_{l-1/2}(k'R) N_{l+1/2}(kR)}, \quad (17)$$

where $k' = \sqrt{k^2 - m^2}$ and $l = 0, 1, \dots$ in three dimensions. The phase shift for fermions is a rather lengthy calculation that is left until Appendix A.

B. Thermal effective action

Using the techniques of the last section we are now ready to calculate what is essentially the difference in the effective action for the true and false vacua ΔW . We refer the reader to [21] for a detailed discussion of heat kernel methods at finite temperature for scalar and spinor fields. The thermal heat kernel K^β can be expressed as an infinite sum of zero temperature heat kernels

$$K^\beta(t | \tau, x; \tau', x') = \sum_{n=-\infty}^{\infty} (\pm)^n K(t | \tau, x; \tau' + \beta n, x') \quad (18)$$

(where \pm is for scalar and spinor fields respectively) and for an ultrastatic spacetime, the heat kernel can be factorised into temporal and spacial parts giving

$$K(t | \tau, x; \tau', x') = \frac{1}{\sqrt{4\pi t}} e^{-\frac{(\tau-\tau')^2}{4t}} K^{(3)}(t | x, x'). \quad (19)$$

It is then possible to show using the above relations that,

$$K^\beta(t) = \frac{\beta}{\sqrt{4\pi t}} \sum_{n=-\infty}^{\infty} e^{-\frac{n^2\beta^2}{4t}} K^{(3)}(t). \quad (20)$$

ΔW is related to the thermal heat kernel $\Delta K^\beta(t)$ for scalar fields by

$$\Delta W = -\frac{1}{2} \int_0^\infty \frac{dt}{t} \text{tr} \Delta K^\beta(t). \quad (21)$$

Substituting (20) into the above equation, we obtain for scalars,

$$\Delta W = -\frac{\beta}{2} \int_0^\infty \frac{dt}{t} \sum_{n=-\infty}^{\infty} e^{-\frac{\beta^2}{4t} n^2} \frac{1}{\sqrt{4\pi t}} \frac{2}{\pi} \int_0^\infty dk e^{-k^2 t} k t \sum_{l=0}^{\infty} (2l+1) \delta_l(k). \quad (22)$$

Then, using the fact that

$$\int_0^\infty t^{-\frac{1}{2}} e^{-\frac{\beta^2}{4t} n^2 - k^2 t} dt = \frac{\sqrt{\pi}}{k} e^{-n\beta k}, \quad (23)$$

we get

$$\Delta W = -\frac{\beta}{2\pi} \int_0^\infty dk \sum_{l=0}^{\infty} (2l+1) \delta_l(k) - \frac{\beta}{\pi} \int_0^\infty dk \sum_{l=0}^{\infty} (2l+1) \delta_l(k) \sum_{n=1}^{\infty} e^{-n\beta k}. \quad (24)$$

The sum over n is standard, leading to the result

$$\Delta W = -\frac{\beta}{2\pi} \int_0^\infty dk \sum_{l=0}^{\infty} (2l+1) \bar{\delta}_l(k) - \frac{\beta}{\pi} \int_0^\infty dk \sum_{l=0}^{\infty} (2l+1) \frac{\delta_l(k)}{e^{\beta k} - 1}. \quad (25)$$

The first term is the zero point energy, that contains the ultraviolet divergences of the theory and hence $\bar{\delta}_l(k)$ (see equation (20) & (13)). The second term is the temperature dependent part. The above expression can be derived using the density of states method

[12]. Thus, upon regulating the nonthermal part, using zeta function regularization and introducing a mass that we let tend to zero at the end of the calculation (see Appendix B), we have

$$\Delta W^N = -\frac{\beta}{2\pi} \int_0^\infty dk \left(\sum_{l=0}^\infty (2l+1) \delta_l(k) - 2\sqrt{\pi} B_1 k - \frac{\sqrt{\pi} B_2}{\sqrt{(k^2 + M_{IR}^2)}} \right) + \frac{\beta B_2}{2\sqrt{4\pi}} \log M_{IR}^2, \quad (26)$$

$$\Delta W^T = -\frac{\beta}{\pi} \int_0^\infty dk \sum_{l=0}^\infty (2l+1) \frac{\delta_l(k)}{e^{\beta k} - 1}, \quad (27)$$

where $\Delta W = \Delta W^N + \Delta W^T$ is the thermal effective action and we are working explicitly in three dimensions. (Note that ΔW is independent of M_{IR}^2 and for the scalar boson, $B_{3/2}$ is zero.)

For fermions the spinor effective action $\Delta W_{(1/2)}$ is related to the heat kernel $\Delta K_{(1/2)}^\beta(t)$ by (twice the scalar result for massive fermions and also a colour factor of three if the top quark is considered)

$$\Delta W_{(1/2)} = \int_0^\infty \frac{dt}{t} \text{tr} K_{(1/2)}^\beta(t). \quad (28)$$

Thus,

$$\Delta W_{(1/2)} = 4\beta \int_0^\infty \frac{dt}{t} \sum_{n=-\infty}^\infty (-1)^n e^{-\frac{\beta^2}{4t} n^2} \frac{1}{\sqrt{4\pi t}} \frac{2}{\pi} \int_0^\infty dk e^{-k^2 t} k t \sum_{j=1/2}^\infty 2(2j+1) \delta_f(k), \quad (29)$$

where $\delta_f = \delta_+ + \delta_-$ (see appendix) and $j = 1/2, 3/2, \dots$ in three dimensions (the factor of four comes from the trace over spinor indices). Applying (23) gives

$$\Delta W_{(1/2)} = \frac{4\beta}{\pi} \int_0^\infty dk \sum_{j=1/2}^\infty 2(2j+1) \delta_f(k) - \frac{8\beta}{\pi} \int_0^\infty dk \sum_{j=1/2}^\infty 2(2j+1) \delta_f(k) \sum_{n=1}^\infty (-1)^n e^{-n\beta k}. \quad (30)$$

Then, summing over n we have

$$\Delta W_{(1/2)} = \frac{4\beta}{\pi} \int_0^\infty dk \sum_{j=1/2}^\infty 2(2j+1) \bar{\delta}_f(k) - \frac{8\beta}{\pi} \int_0^\infty dk \sum_{j=1/2}^\infty 2(2j+1) \frac{\delta_f(k)}{e^{\beta k} + 1}. \quad (31)$$

Of course, we could have guessed this result from looking at (25), taking into account the properties of spinors. It is fairly simple to derive the above equation using the density of states in the same way as in [12], using the spinor phase shift. Thus,

$$\Delta W_{(1/2)}^N = \frac{4\beta}{\pi} \int_0^\infty dk \left(\sum_{j=1/2}^\infty 2(2j+1) \delta_f(k) - 2\sqrt{\pi} B_1 k - \pi B_{3/2} - \frac{\sqrt{\pi} B_2}{\sqrt{(k^2 + M_{IR}^2)}} \right) - \frac{2\beta B_2}{\sqrt{\pi}} \log M_{IR}^2, \quad (32)$$

$$\Delta W_{(1/2)}^T = -\frac{8\beta}{\pi} \int_0^\infty dk \sum_{j=1/2}^\infty 2(2j+1) \frac{\delta_f(k)}{e^{\beta k} + 1}. \quad (33)$$

Note the opposite sign in the zero point energy (nonthermal) contribution to the one loop effective action as compared to the scalar case equation (26).

III. THICKER WALLS

The phase shift method works equally well for any bubble profile, although a differential equation must be solved numerically to find the phase shift. In the general case, one could consider the difference between the phase shift and thin wall phase shift and then add this correction onto the effective action numerically. Alternatively, it is possible to estimate the corrections due to the non-zero thickness of the wall by perturbing about the thin wall case. For example, consider the scalar boson, for which we must solve

$$-r^{-2}(r^2 u')' + m^2 u + \frac{l(l+1)}{r^2} u - k^2 u = -V u, \quad (34)$$

where m is given by equation (2), V is the correction due to a thicker wall and we define R such that $\int_0^\infty r^2 V(r) dr = 0$. The Green's function is

$$G(r, r') = - \begin{cases} kA^{-1} u_1(r) u_2(r') & r < r' \\ kA^{-1} u_2(r) u_1(r') & r > r' \end{cases} \quad (35)$$

and

$$u_1(r) = \begin{cases} j_l(k'r) & r < R \\ Aj_l(kr) - Bn_l(kr) & r > R \end{cases}; \quad u_2(r) = \begin{cases} Cj_l(kr') + Dn_l(kr') & r < R \\ n_l(kr) & r > R \end{cases}, \quad (36)$$

where $k' = \sqrt{k^2 - M^2}$ and $j_l(z) = \sqrt{\frac{\pi}{2}} z^{(1-d)/2} J_{l+(d-1)/2}(z)$ in $d+1$ dimensions.

One then imposes $u \propto j_l$ as $r \rightarrow 0$ and $u \propto Aj_l - B'n_l$ as $r \rightarrow \infty$. Then, the solution is

$$u = u_1 - \int_0^\infty G(r, r') V(r') u(r') r'^2 dr'. \quad (37)$$

Therefore, as $r \rightarrow \infty$

$$u \rightarrow u_1 + kA^{-1} u_2 \int_0^\infty V(r') u_1^2(r') r'^2 dr'. \quad (38)$$

From this it is possible to show that the correction to the phase shift is

$$\delta^{(1)} = -\frac{k}{A^2 + B^2} \int_0^\infty V(r) u_1^2(r) r^2 dr. \quad (39)$$

Then, assuming that the Bessel functions change little as r varies over the bubble wall, they can be Taylor expanded about R , giving

$$\delta^{(1)} \approx -\frac{2kk'}{A^2 + B^2} j_l(k'R) j_l'(k'R) \int_0^R V(r) r^3 dr, \quad (40)$$

where the continuity of u_1 at the bubble wall has been used. For the scalar case,

$$B = -kR^2 (k j_{l-1}(kR) j_l(k'R) - k' j_l(kR) j_{l-1}(k'R)) \quad (41)$$

and

$$A = -kR^2 (k n_{l-1}(kR) j_l(k'R) - k' n_l(kR) j_{l-1}(k'R)). \quad (42)$$

All the terms outside the integral in equation (40) are numerical factors. For reasons discussed in the conclusion we only add the correction onto the thermal part of the effective action, giving

$$\Delta W^{(1)} = \alpha \frac{\beta}{R^3} \int_0^R V(r) r^3 dr \quad (43)$$

where α is given by

$$\alpha = -\frac{1}{\pi} \int_0^\infty dz \sum_{l=0}^\infty \frac{(2l+1)}{e^{\beta z/R} - 1} \frac{2zz'}{A^2 + B^2} j_l(z') j_l'(z'). \quad (44)$$

If one assumes a ‘*tanh*’ like potential $m^2(r)$ for the thicker wall, then $V = m^2(r) - m^2 \approx -m^2/2$ at the bubble wall radius R . Therefore, in terms of the width w of the bubble wall one obtains the approximate result $\Delta W^{(1)} \approx -\alpha \beta m^2 w/2$. We have calculated α numerically and found that it is of order 1 for a range of values of β/R .

IV. RESULTS

The thermal one loop effective action was calculated numerically for fermions. The phase shift is substituted into equations (32) and (33), where it is convenient to change variables $k \rightarrow z = kR$ for the step potential. Then the nonthermal part has only one parameter $\eta = m_f^2 R^2$, where m_f is the mass of the fermion. The thermal part has parameters η and βm_f (given that $\beta/R = \beta m_f / \sqrt{\eta}$) as independent variables.

We work with equations (32) and (33) using a numerical package. For each value of z the function is summed over l (or j), with l increasing up to a given L until the value of the function at z converges. The thermal part of the integral converges due to the exponential damping terms. When considering the nonthermal part of the function, we must check that the integrand has the correct k dependence after making the subtraction of the divergent quantities from the sum over the phase shift. This is a good check verifying that the heat kernel coefficients are correct.

We integrate up to Z chosen to obtain the required accuracy (all results are accurate to 1%). For large values of η (and small βm_f), larger values of Z and L are needed to give convergence. The *arctan* function (from the phase shift) has problems with branches for large values of η (whenever δ hits $\pm\pi$), requiring numerical glueing of the phase shift.

The nonthermal part of the fermion effective action can be written $\beta m_f F(\eta)$. Numerically, $F(\eta)$ fits well to a power law dependence on η (see Fig. 1), giving, in the original variables,

$$\Delta W_{(1/2)}^N = -1.51 \beta m_f^3 R^2 + 0.32 \beta m_f^4 R^3 \quad (45)$$

where we have set the renormalisation scale $\mu = M_{IR} = m_f$ as explained in Appendix C. The nonthermal part is plotted in Fig. 2. The full one loop effective action for fermions plotted against η is in Fig. 3 for various values of the parameter βm_f .

V. CONCLUSION

We have presented a simple method to compute the prefactor in the expression for the bubble nucleation rate, applying this to infinitely thin walls. Analytic corrections due to thicker walls were considered by perturbing about the thin wall case. It is easy to see that these corrections do not effect the B_1 heat kernel coefficient. Using the arguments from Appendix C, where it was shown that we only need to consider the renormalisation of the thin wall bubble, one can ignore the correction from B_2 . Thus, only adding corrections to the thermal part of the effective action should be a good approximation.

In the context of the electroweak phase transition, we would also like to examine the vector bosons, using the method presented. This requires vector spherical harmonics and the relevant boundary conditions to calculate the phase shift. Then a full treatment of all the particle species at the phase transition can be worked out in the thin wall approximation, including analytic expressions for corrections due to thicker walls.

The fermion contribution generally enhances the rate, but for large βm_f (when $\mu = m_f$) it does not and becomes suppressive. In fact, at $\beta m_f = 5.0$ (see figure 3), the sign of the effective action changes for various values of $\eta = m_f R$ (for a fixed bubble wall radius). Choosing $\mu = m_t$ and $m_f = m_t$ (the mass of the top quark) as in [11], then the log term cancels for the fermion determinant (see equation (45)). Baacke and Sürig [11] found a negative contribution (enhance), whereas we find it can also be positive (suppress) for a temperature ($\frac{1}{\beta} = 35\text{GeV}$ with $\beta m_t = 5.0$ and $m_t \approx 175\text{GeV}$) lower than the that at the electroweak phase transition. However, there is no direct method of comparison between the two methods because in [11] the thin wall limit was not considered.

The renormalisation scale can be set by imposing conditions on the effective potential, calculated for constant background fields [12]. In Appendix C it was shown that these conditions on the effective potential (that include the classical and regularised terms) lead to the choice $\mu = M_{IR} = m_f$.

In the case of bubble nucleation, the bubble wall radius is found by extremising an action which includes the effective potential. The three dimensional action for the bounce solution is

$$B = 4\pi\beta R^2\sigma - \frac{4\pi}{3}\beta R^3\epsilon, \quad (46)$$

where σ and ϵ are corrected surface and volume energy densities respectively. The nonthermal part of the effective action (equation (45)) has a similar form and can be absorbed into a redefinition of σ and ϵ . The value of R should be presumably chosen to coincide with the extrema of the new action. Then, the nucleation rate is determined as a function of temperature by ΔW^T .

The method described can also be used to calculate the one loop effective action in general, but in this case the B_0 heat kernel coefficient must be renormalised away in the vacuum energy. The numerical procedure is simple and efficient.

ACKNOWLEDGMENTS

W.N. would like to thank JSPS for Postdoctoral Fellowship for Foreign Researchers No. P01773, where this work was revised and completed.

VI. APPENDIX

A. Fermion phase shift

Here we present the calculation of the spinor phase shift. One must use the Dirac equation separated into radial and angular coordinates and also be careful in the way one works out the eigenvalues of the problem. Starting with

$$(i\gamma \cdot \delta - m)\psi_+ = \lambda\psi_-, \quad (47)$$

$$(i\gamma \cdot \delta + m)\psi_- = -\lambda\psi_+, \quad (48)$$

so that upon squaring the Dirac equation we get the Klein Gordon equation. The radial components are then [17]

$$(E \mp m)g_{\pm} + f'_{\pm} + (j + \frac{3}{2})\frac{f_{\pm}}{r} = \pm\lambda g_{\mp}, \quad (49)$$

$$(E \pm m)f_{\pm} - g'_{\pm} + (j - \frac{1}{2})\frac{g_{\pm}}{r} = \mp\lambda f_{\mp}, \quad (50)$$

where

$$\Psi_{\pm} = \begin{pmatrix} ig_{\pm}Y \\ f_{\pm}\sigma_r Y \end{pmatrix}; \quad \sigma_r = \begin{pmatrix} 0 & -i \\ i & 0 \end{pmatrix}, \quad (51)$$

for $j = l + 1/2$. The solutions are spherical Bessel functions $f_{\pm} = A_{\pm}j_{j\pm\frac{1}{2}}$ and $g_{\pm} = C_{\pm}j_{j\pm\frac{1}{2}}$ (this can be seen easily by substituting (49) into (50)) where the constants are as yet undetermined. On substituting the power series for the Bessel functions into (49) and (50) one finds the relations

$$(E \mp m)C_{\pm} + A_{\pm}k \mp \lambda C_{\mp} = 0, \quad (52)$$

$$(E \pm m)A_{\pm} + C_{\pm}k \pm \lambda A_{\mp} = 0. \quad (53)$$

The correct eigenvalue problem requires mixed boundary conditions [19] (also for a self-adjoint action) leading to $f_+ + g_+ = f_- - g_- = 0$ as $r \rightarrow \infty$. It is also possible to show that there is a symmetry among the solutions such that $f_+ \leftrightarrow f_-$ and $g_+ \leftrightarrow -g_-$. For the calculation we set $E = 0$ and impose the boundary conditions with the above symmetries, noting that $m \rightarrow 0$ as $r \rightarrow \infty$. Using this information, it is possible to show that there are two solutions

$$\tan \delta = \frac{B_+}{A_+}, \quad (54)$$

for $A_+ = \pm C_+$ and $B_+ = \pm D_+$, where B_{\pm} and C_{\pm} are the corresponding constants for $n_{j\pm\frac{1}{2}}$, the irregular solutions, that are spherical Neumann functions.

Then, matching the wavefunction at the junction and performing some algebra, we get the phase shifts,

$$\tan \delta_{\pm} = \frac{(k \pm m) J_j(kR) J_{j+1}(k'R) - k' J_j(k'R) J_{j+1}(kR)}{(k \pm m) N_j(kR) J_{j+1}(k'R) - k' J_j(k'R) N_{j+1}(kR)}. \quad (55)$$

where all symbols have their usual meanings as in the rest of the paper.

The $j = l - 1/2$ modes have symmetry such that $f_{\pm} \leftrightarrow g_{\pm}$ changes the boundary conditions and equations into the $j = l + 1/2$ case. Thus we have the above phase shifts with a total degeneracy $2(2j + 1)$, where $j = 1/2, 3/2, \dots$. All results can be generalised to the four dimensional case.

B. Numerical zeta function regularisation

Consider the finite temperature case. The nonthermal part of the heat kernel is

$$\Delta K_0(t) = \frac{\beta}{\sqrt{(4\pi t)}} \frac{2}{\pi} \int_0^{\infty} dk k e^{-(k^2 + M^2)t} \sum_{\gamma} \delta_{\gamma}(k) t, \quad (56)$$

where all symbols have the same conventions as in the rest of the paper and we have introduced a mass term M . The zeta function is then

$$\Delta \zeta_0(s) = \frac{\beta}{\sqrt{(4\pi)}} \frac{2}{\pi} \frac{\Gamma(s + \frac{1}{2})}{\Gamma(s)} \int_0^{\infty} dk k (k^2 + M^2)^{-s - \frac{1}{2}} \sum_{\gamma} \delta_{\gamma}(k). \quad (57)$$

The integral converges for $s > 1$. In order to apply the zeta function to numerical work, we subtract terms from the asymptotic expansion of the heat kernel and define

$$P(s) = \frac{2}{\pi} \frac{\beta}{\sqrt{(4\pi)}} \frac{\Gamma(s + \frac{1}{2})}{\Gamma(s)} \int_0^{\infty} dk k (k^2 + M^2)^{-s - \frac{1}{2}} \left\{ \sum_{\gamma} \delta_{\gamma} - 2\sqrt{\pi} B_1 k - \pi B_{3/2} - \sqrt{\pi} \frac{B_2}{k} \right\}. \quad (58)$$

Performing the integration over k , and adding back the subtracted terms, one finds

$$\Delta \zeta_0(s) = P(s) + \frac{\beta}{2\sqrt{\pi}} M^{2-2s} \frac{B_1}{s-1} + \frac{\beta}{2\sqrt{\pi}} \frac{\Gamma(s - \frac{1}{2})}{\Gamma(s)} M^{1-2s} B_{3/2} + \frac{\beta}{2\sqrt{\pi}} M^{-2s} B_2. \quad (59)$$

This is a regular function at $s = 0$. Taking the derivative with respect to s (for $s = 0$) and the limit $M \rightarrow 0$, we obtain

$$\Delta \zeta'_0(0) = \frac{\beta}{\pi} \int_0^{\infty} dk \left(\sum_{\gamma} \delta_{\gamma} - 2\sqrt{\pi} B_1 k - \pi B_{3/2} - \frac{\sqrt{\pi} B_2}{\sqrt{(k^2 + M_{IR}^2)}} \right) - \frac{\beta B_2}{\sqrt{4\pi}} \log M_{IR}^2, \quad (60)$$

where M_{IR} is an infrared cutoff. It is important to note that if one subtracts the difference between $\Delta \zeta'_0(0)$ for different values of infrared cutoff (M_A and M_B say) and using the fact that

$$\int_0^{\infty} dk \left(\frac{1}{\sqrt{k^2 + M_A^2}} - \frac{1}{\sqrt{k^2 + M_B^2}} \right) = \log \frac{M_B}{M_A}, \quad (61)$$

it is clear that this difference is zero. Thus, equation (60) is independent of M_{IR} .

C. Renormalisation

The renormalisation scale μ represents an arbitrary parameter that can be expressed in terms of other constants by imposing conditions on the effective potential (see [22] for example). We shall show that the usual renormalisation conditions for the effective potential,

$$\begin{aligned} V'(\phi_{vac}) &= 0, \\ V''(\phi_{vac}) &= m_h, \end{aligned} \quad (62)$$

where ϕ_{vac} is the classical vacuum expectation value and m_h is the mass of the Higgs field, give the optimal choice, removing the logarithmic term.

The first two terms in the zero point energy (45) come from the finite, subtracted, part of the effective action (see equation (58)). A similar approach was used in [11], where the divergent effective action was regularised by subtracting terms proportional to 1st and 2nd powers of the background potential, leaving a finite contribution to the fluctuation determinant. The two divergent terms were then regulated by using a momentum cutoff and renormalised by applying conditions on the propagators. This procedure is equivalent to the subtraction of the heat kernel coefficients up to and including B_2 (see equation (58)). However, zeta function regularisation is unusual, as compared with most regularisation schemes, in that it does not need infinite counter terms. Thus, in equation (60) only the last term, containing the logarithm, requires renormalisation.

The effective potential $V = V_0 + V_1$ will be defined

$$V = \int \beta d^3x \left[\frac{1}{2}(m_h^2 + \delta m_h^2)\phi^2 - (g + \delta g)\phi^3 + \frac{1}{4}(\lambda + \delta\lambda)\phi^4 \right] - \frac{2\beta B_2}{\sqrt{\pi}} \log \frac{M_{IR}^2}{\mu^2}, \quad (63)$$

where the terms in the square brackets make up the classical potential (including counterterms), the last term is the ζ -regularised 1-loop contribution with

$$B_2 = \Delta\zeta_0(0) = \frac{\beta}{(4\pi)^{3/2}} \int d^3x \frac{1}{2} m_f^4 \phi^4(\vec{x}), \quad (64)$$

and we have included the renormalisation scale μ (see equation (11)).

In our case the renormalisation must be applied to a step function field configuration, but the ultraviolet divergences are independent of the background profile. This is intuitively obvious because $k \rightarrow \infty$ equates to the short distance behaviour of the theory. Thus, the B_2 heat kernel coefficient ($\propto \phi^4(\vec{x})$) need only be considered for $\phi(\vec{x}) = constant$, i.e. the effective potential.

By applying the renormalisation conditions (62) to the effective potential, it is simple to show that the counter terms are given by $\delta m_h^2 = \delta g = 0$ and

$$\delta\lambda = \frac{m_f^4}{\sqrt{2}\pi^2} \log \frac{M_{IR}^2}{\mu^2}. \quad (65)$$

On substituting the above counterterms into the effective potential it is clear that the logarithmic term will cancel. Naturally, for our numerical procedure we can choose $M_{IR} = m_f$ because it was shown in Appendix B that the infrared cutoff was independent of the result (equation (60)).

With our choice of renormalisation we can compare with a similar work [12], where the scalar Higgs field was investigated. In the case of the thin wall limit they only considered the surface free energy. However, comparing with our zero point surface energy contribution, for a scalar boson [23], we find it is of a similar order of magnitude and also suppresses the nucleation rate. This contribution is considerably smaller than that made by a fermion with a Yukawa coupling which, generally, enhances the nucleation rate.

REFERENCES

- [1] S. Coleman, Phys. Rev. D 15 (1977) 2929; C. G. Callan and S. Coleman, *ibid.* D 16 (1977) 1762.
- [2] V. Zarikas, Phys. Lett. B 384 (1996) 180.
- [3] G. W. Anderson and L. J. Hall, Phys. Rev. D 45 (1992) 2685.
- [4] W. Naylor, in progress.
- [5] M. Gleiser, G. C. Marques and R. O. Ramos, Phys. Rev. D 48 (1995) 1571.
- [6] J. Garriga, Phys. Rev. D 49 (1994) 5497.
- [7] J. Kripfganz, A. Laser, and M. G. Schmidt, Nucl. Phys. B 433 (1995) 467.
- [8] S. Coleman, Aspects of Symmetry (Cambridge University Press, Cambridge, England, 1985).
- [9] J. Baacke and V.G. Kiselev, Phys. Rev. D 48 (1993) 5648.
- [10] J. Baacke, Phys. Rev. D 52 (1995) 6760.
- [11] J. Baacke and A. Sürig, Phys. Rev. D 53 (1996) 4499.
- [12] C. L. Y. Lee, Phys. Rev. D 49 (1994) 4101; D. E. Brahm and C. L. Y. Lee, Phys. Rev. D 49 (1994) 4094.
- [13] J. Schwinger, Phys. Rev. 94 (1954) 1362.
- [14] G. Münster and S. Rotsch, Eur. Phys. J. C 12 (2000) 161.
- [15] G. Münster, A. Strumia and N. Tetradis, Phys. Lett. A 271 (2000) 80.
- [16] A. D. Linde, Phys. Lett. 70 B, 306 (1977); 100 B (1981) 37.
- [17] L. I. Schiff, Quantum Mechanics (McGraw-Hill, Singapore 1968).
- [18] J. S. Dowker and J. Critchley, Phys. Rev. D 13 (1976) 3224.
- [19] I. G. Moss, Quantum theory, Black Holes and Inflation (Wiley, 1996)
- [20] M. Bordag and D. V. Vassilevich, J. Phys. A 32 (1999) 8247; I. G. Moss, Phys. Lett. B 491 (2000) 203.
- [21] J. S. Dowker and J. P. Schofield, Nucl. Phys. B 327 (1989) 267; Y. V. Gusev and A. I. Zelnikov, Phys. Rev. D 59 (1999) 024002.
- [22] A. Berkin, Phys. Rev. D 46 (1992) 1551.
- [23] W. Naylor, Ph. D. Thesis (University of Newcastle Upon Tyne, 2001)

FIGURES

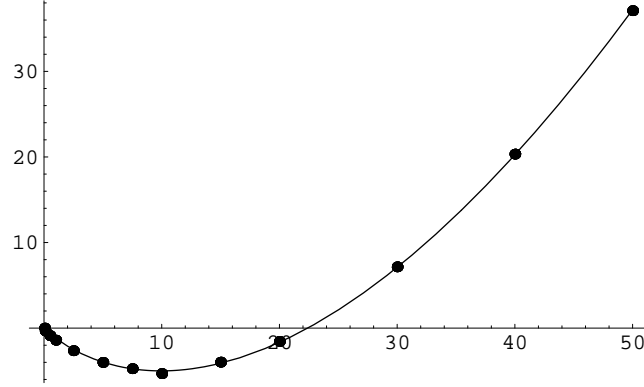


FIG. 1. Fit of the nonthermal part of the one loop contribution to the fermion effective action $\Delta W_{(1/2)}^N$, plotted against η .

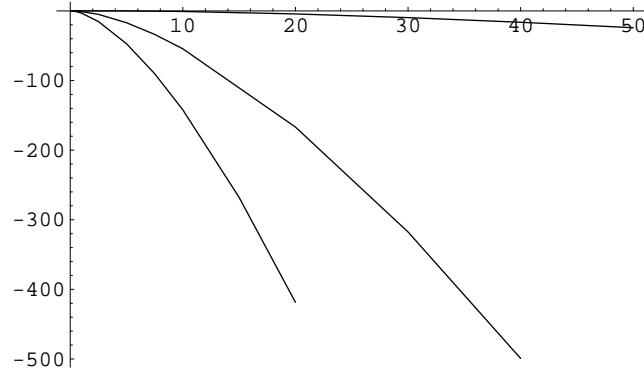


FIG. 2. The thermal part of the one loop contribution to the fermion effective action $\Delta W_{(1/2)}^T$, plotted against η for values of βm_f (from bottom to top); 0.5, 1.0 & 5.0.

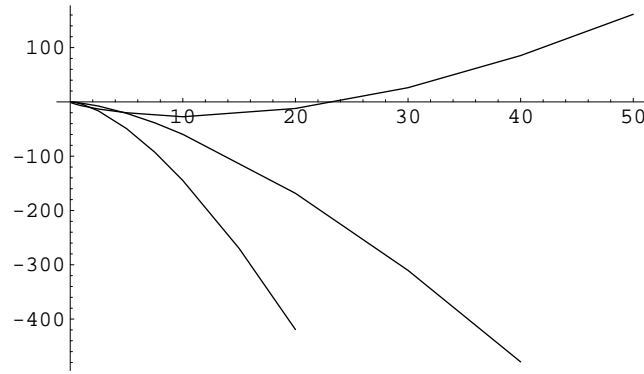


FIG. 3. The full one loop contribution to the fermion effective action $\Delta W_{(1/2)}$, plotted against η for values of βm_f (from bottom to top); 0.5, 1.0 & 5.0.